ARTICLE

Development of a Pharmacokinetic Model Describing Neonatal Fc Receptor-Mediated Recycling of HL2351, a Novel Hybrid Fc-Fused Interleukin-1 Receptor Antagonist, to Optimize Dosage Regimen

Lien Ngo[1,†], Jaeseong Oh[2,†], Anhye Kim[3], Hyun-moon Back[4], Won-ho Kang[1], Jung-woo Chae[1], Hwi-yeol Yun[1,*] and Howard Lee[2,5,*]

HL2351 (hIL-1Ra-hyFc) is a novel recombinant protein formed by the fusion of two human interleukin-1 receptor antagonist components into one antibody-derived fragment crystallizable portion. Although HL2351 has a pharmacological mechanism of action similar to that of anakinra as a commercialized biopharmaceutical drug, HL2351 has been desired to reduce the dose frequency and improve therapeutic efficacy due to its long circulation half-life. In this study, we aimed to develop a population pharmacokinetic (PK) model for HL2351 using a neonatal Fc receptor (FcRn)–mediated recycling model based on a quasi-steady-state approximation of target-mediated drug disposition (TMDD) for the description of interactions between the drug and FcRn. FcRn recycling was expected in the case of HL2351 because of PK related to the antibody portion. A TMDD model was also applied to describe interactions of IL1R with HL2351 or anakinra. PK data were collected from a phase I study conducted in six groups (1, 2, 4, 8, 12 mg/kg HL2351 and 100 mg anakinra single subcutaneous administration; $n = 8$ per group). In consequence, the PK of anakinra and HL2351 following administration of multiple doses at different dosages were simulated. Optimized doses were considered based on average concentrations of IL1R bound to anakinra and HL2351. HL2351 at doses of 326 mg or 4.267, 4.982, 5.288, 5.458, or 5.748 mg/kg once weekly or HL2351 at 1726 mg or 21.92, 26.86, 29.10, 30.36, or 32.53 mg/kg once biweekly would have similar therapeutic effects with anakinra at a dose of 100 mg or 1, 2, 3, 4, or 8 mg/kg administered once daily, respectively.

Study Highlights

WHAT IS THE CURRENT KNOWLEDGE ON THE TOPIC?
☑ Anakinra, a recombinant human interleukin-1 receptor antagonist, has a short half-life (4–6 hours); therefore, it requires daily administration. HL2351 (hIL-1Ra-hyFc) has been developed as an alternative medication for anakinra because of its long half-life characteristics (27.21–45.28 hours). However, there was a limitation of prediction for HL2351 therapeutic equivalent doses to anakinra doses.

WHAT QUESTION DID THIS STUDY ADDRESS?
☑ The neonatal Fc receptor (FcRn)–mediated recycling target-mediated drug disposition (TMDD) model for HL2351, which characterized both target-mediated disposition and FcRn-mediated recycling, and a TMDD model for anakinra, in humans, was developed in this study.

HL2351 dosage regimen that mimicked the therapeutic actions of anakinra was estimated by a model-based approach.

WHAT DOES THIS STUDY ADD TO OUR KNOWLEDGE?
☑ HL2351 at doses of 326 mg or 4.267, 4.982, 5.288, 5.458, or 5.748 mg/kg once weekly or 1726 mg or 21.92, 26.86, 29.10, 30.36, or 32.53 mg/kg once biweekly could mimic the therapeutic effects of anakinra at doses of 100 mg or 1, 2, 3, 4, or 8 mg/kg once daily, respectively.

HOW MIGHT THIS CHANGE CLINICAL PHARMACOLOGY OR TRANSLATIONAL SCIENCE?
☑ The estimated dosage could be applied when conducting clinical trials for HL2351. In addition, the developed model could be expanded for other monoclonal antibody drugs and antibody conjugated drugs.

Interleukin-1 (IL1) is a proinflammatory cytokine produced by monocytes and macrophages, which plays an important role in inflammatory processes and the induction of the immune response.[1–3] Once bound to IL1 receptor (IL1R), IL1 triggers a cascade of inflammatory mediators and attracts monocytes, macrophages, and neutrophils to the area of

†Lien Ngo and Jaeseong Oh contributed as much to this work as the first author.

¹College of Pharmacy, Chungnam National University, Daejeon, Republic of Korea; ²Department of Clinical Pharmacology and Therapeutics, Seoul National University College of Medicine and Hospital, Seoul, Republic of Korea; ³Department of Clinical Pharmacology and Therapeutics, CHA Bundang Medical Center, CHA University, Seongnam, Gyeonggi-do, Republic of Korea; ⁴Department of Pharmaceutics, Ernest Mario School of Pharmacy, Rutgers, The State University of New Jersey, New Brunswick, New Jeresy, USA; ⁵Department of Molecular Medicine and Biopharmaceutical Sciences, Graduate School of Convergence Science and Technology, Seoul National University, Seoul, Republic of Korea. *Correspondence: Hwi-Yeol Yun (hyyun@cnu.ac.kr) and Howard Lee (howardlee@snu.ac.kr)

inflammation. This stimulus activates macrophages and promotes the growth and proliferation of T cells and B cells. Overproduction of IL1 is implicated in a variety of acute and chronic inflammatory conditions as well as autoimmune disorders (e.g., rheumatoid arthritis [RA], neuropathic pain, Alzheimer's disease).[1–3] The bioactivity of IL1 is inhibited by the IL1 receptor antagonist (IL1Ra), which competitively binds to IL1R without inducing signal transduction, and the IL1 soluble receptor, which binds to IL1 and reduces the free concentration of soluble cytokine, thus hampering interactions between IL1 and IL1R.

Targeting IL1 began in 1993 with anakinra (Kineret; Amgen, Thousand Oaks, CA), a recombinant form of human IL1Ra that was produced using an *Escherichia coli* expression system. Currently, anakinra is approved for use alone or in combination with other anti-inflammatory drugs for the treatment of RA, cryopyrin-associated periodic syndromes (CAPS), and Still's disease.[4,5] Because of its short half-life ($t_{1/2}$) of ~4 to 6 hours, anakinra requires daily administration to maintain therapeutic levels.[4–6] The safety and efficacy of anakinra for the treatment of inflammatory diseases have been examined in many clinical trials. However, daily administration and injection-site reactions make anakinra challenging for patients and scientists.[7] Therefore, a novel compound with a longer half-life that is mechanistically similar to anakinra is highly desirable.

HL2351 (hIL-1Ra-hyFc) is a novel recombinant protein formed by the fusion of two human IL1Ra components (that are active ingredients of anakinra) into one antibody-derived fragment crystallizable (Fc) portion. HL2351 was developed by Handok Inc. (Seoul, Republic of Korea). The Fc hinge region of HL2351 is derived from human immunoglobulin D (as a flexible antibody), and the remaining compound is derived from human immunoglobulin G4 (IgG4), which is less susceptible to antibody-dependent cellular cytotoxicity and complement-dependent cytotoxicity. HL2351 remains in the body longer than anakinra because of its high molecular weight (~97 kDa); thus it is less likely to be eliminated by renal glomerular filtration, and because of its IgG4-sourced Fc portion, HL2351 can bind to the neonatal Fc receptor (FcRn), thus protecting it from endosomal metabolic catabolism. FcRn is expressed in the vascular endothelial cells of a wide variety of tissues and maintains immunoglobulin G (IgG) homeostasis because it allows IgG to be recirculated throughout the body.[8–13] Consequently, the half-life for IgG is ~18 to 21 days, which is substantially longer than other proteins of similar molecular weight.[14–22]

Population pharmacokinetic (PopPK) models of a variety of monoclonal antibodies (mAbs) have been developed in previous studies.[23–28] However, most studies characterize only the targeted-mediated drug disposition (TMDD) process rather than the FcRn-mediated recycling process. A PopPK model for rituximab in rats was developed by Kagan *et al.*[28] this is the only PopPK model that includes mAb recycling. However, the interaction kinetics between the mAb and FcRn that result in recycling has not yet been characterized. In this study, we developed a PopPK model to describe the pharmacokinetics (PK) of HL2351 in humans. For the first time, we characterized both the TMDD (i.e., interactions between the IL1Ra portion and its therapeutic cell membrane target, IL1) and FcRn-mediated recycling (i.e., interactions between the IgG4-sourced Fc portion and FcRn) of HL2351. Moreover, we developed a quasi-steady-state (QSS) TMDD PK model for anakinra in humans. The PK of HL2351 and anakinra following the administration of multiple doses in humans were simulated through a PopPK-based approach at different doses. Finally, we identified HL2351 dosage regimens that mimic the therapeutic actions of anakinra for the treatment of RA, CAPS, and Still's disease.

METHODS
Materials and PK data collection
Kineret (anakinra) was purchased as a 100 mg solution (150 mg/ml) in a prefilled syringe from Sobi, Inc (Waltham, MA). HL2351 was received from Handok Inc. Study design, sample collection, and sample analysis were described in detail in our recent publication.[29]

PK data were collected from a phase I clinical trial (NCT02175056) approved by the Institutional Review Board of Seoul National University Hospital, Seoul, Republic of Korea. All participants provided written informed consent, and the study was conducted in accordance with the principles of the Declaration of Helsinki and International Council for Harmonisation Good Clinical Practice. Healthy Korean men aged 20 to 45 years were eligible for this study after assessment of vital signs, 12-lead electrocardiogram tests, laboratory testing, and physical examinations. Participants were randomly divided into six groups ($n = 8$ per group) in which they received a single subcutaneous (s.c.) dose of HL2351 (1, 2, 4, 8, or 12 mg/kg) or anakinra (100 mg). Blood samples were collected at predetermined timepoints, up to 672 hours postadministration for HL2351, and up to 48 hours postadministration for anakinra; samples were stored at 4°C.[29] The serum concentrations of HL2351 and anakinra were determined by a validated enzyme-linked immunosorbent assay[29,30] (as described in the **Supplementary Materials**).

Model structure for PKs of HL2351 and anakinra
A schematic-integrated PK model for HL2351 in humans is presented in **Figure 1a**. The TMDD and FcRn-mediated recycling model were designed to characterize interactions between HL2351 and its receptor target IL1R and between HL2351 and FcRn, respectively. Notations are defined in the **Figure 1** legend. The reversible binding of free unbound HL2351 (D_{free1}) in the distribution space to FcRn, followed by its release back to the central compartment (K_{rec}), protected the mAb from intracellular catabolism and was designated "FcRn-mediated recycling." The reversible binding of free unbound HL2351 (D_{free2}) at the central compartment to IL1R, followed by its dissociation into D_{free2} or degradation (K_{deg2}), was designated as "TMDD." A schematic PK model of anakinra in humans, which characterizes the TMDD of anakinra as a result of its binding to IL1R, is presented in **Figure 1b**.

QSS approximations for drug-target interactions
Production of the drug–target complexes (FcRn–D, IL1R–D, and IL1R–D_A) follows second-order kinetics, with the rate constant K_{on}. Dissociation of the complex back to the free drugs and its targets follows first-order kinetics, with the

FcRn-Mediated PK Model and Dosage Regimen for HL2351
Ngo et al.

586

(a)

(b)
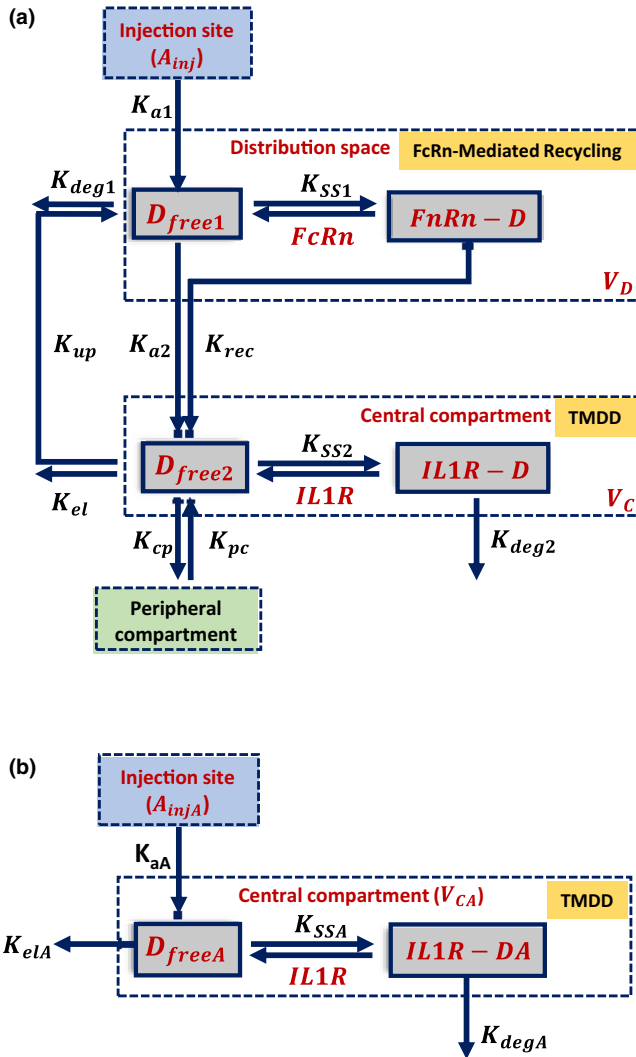
Figure 1 Schematic pharmacokinetic models of (**a**) TMDD and FcRn-mediated recycling of HL2351 in humans and (**b**) TMDD of anakinra in humans. HL2351 was transported from the injection site (Dose) to the distribution space (rate constant K_{a1}). Therein, a part of HL2351 (D_{free1}) was reversibly bound to FcRn to form a FcRn–D complex, which could dissociate into D_{free1} or be transported to the central compartment (rate constant K_{rec}). The remaining D_{free1} was either moved directly to the central compartment (rate constant K_{a2}) or degraded (rate constant K_{deg1}). At the central compartment, a portion of free HL2351 (D_{free2}) bound reversibly to IL1R to form a IL1R–D complex, which then dissociated into D_{free2} or degraded (rate constant K_{deg2}). Another portion of D_{free2} was either taken up into the distribution space (rate constant K_{up}) or intercompartmental transported (rate constants K_{cp} and K_{pc}). The remaining D_{free2} was eliminated from the body (rate constant K_{el}). All notations for anakinra are identical to those used for HL2351, except for the letter "A" in the subscript, which represents anakinra. FcRn, neonatal Fc receptor; TMDD, target-mediated drug disposition.

dissociation rate constant K_{off}. These interactions are described in Eqs. 1–3.

$$D_{free1} + FcRn \underset{K_{off1}}{\overset{K_{on1}}{\rightleftarrows}} FcRn-D \qquad (1)$$

$$D_{free2} + IL1R \underset{K_{off2}}{\overset{K_{on2}}{\rightleftarrows}} IL1R-D \qquad (2)$$

$$D_{freeA} + IL1R \underset{K_{offA}}{\overset{K_{onA}}{\rightleftarrows}} IL1R-D_A \qquad (3)$$
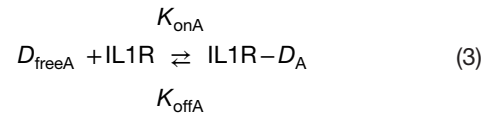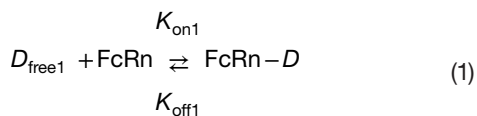
The numbers 1 and 2 in the subscripts denote equations that are relevant to the interactions of HL2351 with FcRn and HL2351 with IL1R, respectively. The letter "A" in the subscript denotes equations relevant to anakinra.

TMDD is the phenomenon whereby a drug binds with a high affinity to its pharmacological target (ligand or receptor), and the binding significantly influences drug disposition. The binding of HL2351 or anakinra with IL1R is a pure TMDD process. Although FcRn is not a therapeutic target of HL2351, the interaction between HL2351 and FcRn follows the kinetics of a TMDD process in which the recycling rate constant K_{rec} is related to the degradation rate constant of a complex in a TMDD process (e.g., K_{deg2}). For convenience, interaction kinetics between HL2351 and FcRn will also be referred to as TMDD kinetics.

A full TMDD model, as well as approximation TMDD models (e.g., quasi-equilibrium, QSS, and Michaelis–Menten approximations) have been previously described in detail.[31–34] In the present study, a QSS approximation was applied. The main assumption used to derive the QSS approximation was that the concentration of the free unbound drug, its target, and its drug–target complex are in QSS condition; thus, the concentration of the complex is constant. The QSS model simplifies the full TMDD model by introducing QSS constants (K_{SS1}, K_{SS2}, or K_{SSA}), the total (bound and unbound) drug concentration/amount (C_{tot1}, C_{totA}, or A_{tot2}), and the total (bound and unbound) receptor concentration/amount (C_{IL1R_t} or A_{FcRn_t}).

Accordingly, the number of free HL2351 in the distribution space (A_{Dfree1}; unbound to FcRn) was derived from total HL2351 (A_{tot1}) as described in Eq. 4; concentrations of free HL2351 (C_{Dfree2}; unbound to IL1R) or free anakinra (C_{DfreeA}; unbound to IL1R) in the central compartment were, respectively, derived from total concentration of HL2351 (C_{tot2}) or anakinra (C_{totA}), respectively, as described in Eqs. 5 and 6.

$$A_{Dfree1} = \frac{(A_{tot1} - A_{FcRn\_t} - AK_{SS1}) + \sqrt{\left[(A_{tot1} - A_{FcRn\_t} - AK_{SS1})^2 + 4 \times AK_{SS1} \times A_{tot1}\right]}}{2} \qquad (4)$$

$$C_{Dfree2} = \frac{(C_{tot1} - C_{IL1R\_t} - K_{SS2}) + \sqrt{\left[(C_{tot} - C_{IL1R\_t} - K_{SS2})^2 + 4 \times K_{SS2} \times C_{tot2}\right]}}{2} \qquad (5)$$

$$C_{DfreeA} = \frac{(C_{totA} - C_{IL1R\_t} - K_{SSA}) + \sqrt{\left[(C_{totA} - C_{IL1R\_t} - K_{SSA})^2 + 4 \times K_{SSA} \times C_{totA}\right]}}{2} \qquad (6)$$

Application of using QSS approximation to describe the drug–target interactions and model codes for the nonlinear mixed effect model (NONMEM) in the modeling PK of

anakinra and HL2351 is provided in the **Supplementary Materials**.

PopPK analyses

PopPK analyses for HL2351 and anakinra were conducted using a software package for nonlinear mixed effects modeling (NONMEM version 7.3.0; ICON Development Solutions, Hanover, MD) and executed through the Perl-speaks-NONMEM (PsN) software tool (version 4.4.0) using Pirana.[35] The first-order conditional estimation method with the interaction option method was used for each step during model development. The final model was selected by comparing the objective function value using the likeli-hood ratio test within NONMEM at a 5% significance level, the goodness-of-fit plots, and the precision of estimates. The selection and evaluation steps for the final model are provided in the **Supplementary Materials**.

Dosage regimen for HL2351

The dosage regimen for HL2351 was estimated by the PopPK model-based approach. One thousand repli-cates were performed using the $SIMULATION function in NONMEM and executed through the PsN software tool using Pirana.[35] PK parameters, individual random effects, and residual random effects for anakinra and HL2351 were assumed to be consistent with their respective observed data. The average serum concentrations of HL2351 bound to IL1R (C_{IL1R-D}) and anakinra bound to IL1R ($C_{IL1R-DA}$), which represented therapeutic effects during one dosing interval at the steady state ($\overline{C_{b_ss}}$) were used as a criterion. The assumption was that if the $\overline{C_{b\_ss}}$ of HL2351 reached the $\overline{C_{b\_ss}}$ of anakinra, HL2351 and anakinra would have similar therapeutic effects.

First, the PK profiles of each drug were simulated (n = 1000 replicates) during one dosing interval in steady-state conditions following multiple doses at different dosage regimens. The dosages for anakinra were 100 mg/day or 1, 2, 3, 4, or 8 mg/kg administered once daily. These were estimated in accordance with the product information for anakinra (Kineret; summarized in **Table S1**).[4,5] PK data were estimated at week 5 postadministration to ensure steady-state conditions. The dosages for HL2351 were 1, 3, 6, 9, 12, or 18 mg/kg once weekly or 1, 6, 12, 18, 24, or 30 mg/kg once biweekly. PK data were estimated at week 29 postad-ministration to ensure steady-state conditions.

Second, $\overline{C_{b\_ss}}$ of HL2351 and anakinra at each dosage regimen were calculated, as represented in Eq. 7.

$$\overline{C_{b\_ss}} = \frac{AUC_{b\_ss}}{\tau} \qquad (7)$$

In this equation, AUC_{b_ss} is the area under the concentra-tion-time curve during one dosing interval at steady-state conditions and τ is one dosing interval time (τ = 24 hours for anakinra, τ = 168 hours for HL2351 administered once weekly, and τ = 336 hours for HL2351 administered once biweekly).

Third, the relationship between the administered dose and $\overline{C_{b\_ss}}$ of HL2351 was fitted in accordance with the Hill equation, as provided in Eq. 8 using Origin (version 2018).

$$\overline{C_{b\_ss}} = C_{max} \times \frac{Dose^n}{Dose_{50}^n + Dose^n} \qquad (8)$$

In this equation, C_{max}(nM) is the maximum value of $\overline{C_{b\_ss}}$, Dose(mg/kg) is the administered HL2351 dose, $Dose_{50}$(mg/kg) is the administered HL2351 dose at which $\overline{C_{b\_ss}}$ of HL2351 is 50% of the C_{max}, and n is the Hill coefficient.

RESULTS

PK study design

PK profiles of anakinra following a single injection (100 mg) and PK profiles of HL2351 following a single injection (1, 2, 4, 8, or 12 mg/kg) were described in detail in our previous study.[29] Briefly, HL2351 was absorbed slowly (with mean time to reach maximum concentration (T_{max}) of 36 hours) and remained in the body up to 240 to 336 hours post-administration. In contrast, concentrations of anakinra declined rapidly; it remained in the body up to 24 to 48 hours postadministration. The mean $t_{1/2}$ of anakinra and HL2351 were 3.97 hours and 27.21 to 45.28 hours, respectively. Compared with anakinra, HL2351 remained in the body ~7-fold to 10-fold longer (55.8–77.36 hours vs. 7.89 hours).

PopPK analysis

Parameter estimates, interindividual variabilities, residual random effects, and relative standard errors for HL2351 and anakinra are listed in **Table 1** and **Table S2**, respec-tively. PK parameters were estimated with small relative standard errors, except for parameters that are relevant to binding kinetics between the drug and its receptors (106.3% for AK_{SS1}; 95.1% for A_{FcRn_t}; 78.0% for C_{IL1R_t}; 68.2% for K_{SS2} of HL2351; and 116.9% for C_{IL1R_t} of anak-inra). Moreover, the low shrinkage values indicated that the observed data were sufficient to precisely estimate the individual parameters.

Basic goodness-of-fit plots of the final models for HL2351 and anakinra are depicted in **Figure S1**; these plots show that the individual and population obser-vations were well fitted. The population and individual post hoc predictions were distributed around the line of identity without systematic bias. Moreover, conditional weighted residuals for the population-predicted serum concentrations were generally distributed around zero and were symmetric. Only 23 of 472 (4.9%) and 2 of 93 (2.2%) conditional weighted residual values of HL2351 and anakinra, respectively, were outside of the range of [−2, +2]. According to the developed PopPK models, QSS constants for the binding of IL1R with HL2351 or anakinra were estimated to be 14.5 nM (K_{SS2}) and 0.750 nM (K_{SSA}), respectively. The total active concentrations of IL1R bound and unbound to HL2351 or anakinra were 2.23 nM and 1.54 nM, respectively. Lastly, the total active amount of FcRn bound and unbound to HL2351 was 749 nmol (**Table 1** and **Table S2**).

Population model evaluation

Figure 2 shows visual predictive check plots for predict-ing the distributions of HL2351 and anakinra concentrations using the final model. The observed concentrations were

Table 1 Parameter estimates for HL2351 after a single subcutaneous injection of HL2351 at a dose range of 1 to 12 mg/kg from the final model and results of bootstrap validation (*n* = 1,000)

Parameter (unit)	Description	Observed data			Bootstrap replicates	
		Median	RSE (%)	Shrinkage (%)	Median	2.5–97.5th
K_{a1} (1/h)	Absorption rate constant of drug from injection site	1.21	28.9	–	1.20	0.851–1.72
AK_{SS1} (nmol)	Equilibrium dissociation constant of drug and FcRn binding	237	106	–	199	33.4–906
A_{FcRn_t} (nmol)	Total active amount of FcRn	749	95.1	–	786	378–1369
K_{a2} (1/h)	Ka of drug from absorption site to central compartment	0.0171	38.3	–	0.0166	0.00752–0.0246
K_{rec} (1/h)	Ka of drug recycled from absorption site to central compartment due to its binding with FcRn	0.0338	50.6	–	0.0319	0.0208–0.0538
K_{deg1} (1/h)	Degradation rate of drug at absorption site	0.0264	39.8	–	0.0292	0.0171–0.0586
CL/F (L/h)	Apparent clearance of drug at central compartment	0.208	36.9	–	0.194	0.036–0.262
Vc/F (L)	Apparent distribution of drug at central compartment	11.3	24.2	–	10.6	6.98–13.3
Q/F (L/h)	Apparent inter-compartment clearance of drug	0.0288	33.6	–	0.0289	0.0188–0.0368
Vp/F (L)	Apparent distribution of drug at peripheral compartment	5.06	FIX	–	5.06	5.06–5.06
K_{deg2} (1/h)	Degradation rate of drug-target complex at central compartment	0.206	FIX	–	0.206	0.2060.206
C_{IL1R_t} (nmol/L)	Total active concentration of target at central compartment	2.23	78.0	–	2.30	0.814–14.6
K_{SS2} (nmol/L)	Dissociation constant of drug and target binding	14.5	68.2	–	13.7	4.122–74.5
K_{up} (1/h)	Uptake rate constant of drug from central back to absorption site	0.00952	FIX	–	-	–
Alag (h)	Lag time	0.312	27.9	–	0.312	0.208–0.409
Interindividual variability (%)						
K_{a1}	Interindividual variability of K_{a1}	97.4	27.6	13.5	94.3	66.9–120
K_{a2}	Interindividual variability of K_{a2}	72.4	35.9	12.4	72.9	49.8–105
K_{rec}	Interindividual variability of K_{rec}	33.2	59.5	39.8	33.2	16.2–52.6
K_{deg1}	Interindividual variability of K_{deg1}	27.5	72.0	36.5	27.3	7.89–56.7
K_{up}	Interindividual variability of K_{up}	90.4	32.8	24.8	89.9	28.1–130
CL/F	Interindividual variability of CL/F	22.9	65.4	36.7	54.7	22.4–79.2
Alag	Interindividual variability of Alag	55.5	69.5	22.6	23.2	11.5–65.7
Residual variability						
Additive (nmol/L)		0.184	35.4		0.181	0.120–0.240
Proportional (%)		11.5	4.3		11.1	9.79–12.8

RSE, relative standard error.

all within the 5th to 95th percentiles of the simulated concentrations. Moreover, most median observed values were within the 95% confidence interval of the median predicted values obtained by simulation. Results of the bootstrap analysis are listed in **Table 1** and **Table S2**; parameter estimates from the final model for the observed data were in close agreement with median values of those estimated from bootstrap replicates, indicating that the NONMEM parameter estimates of the final model were unbiased.

Dosage regimen for HL2351

Simulated PK profiles of HL2351 and anakinra during one dosing interval at steady state following different dosage regimens are illustrated in **Figure 3a**. The means
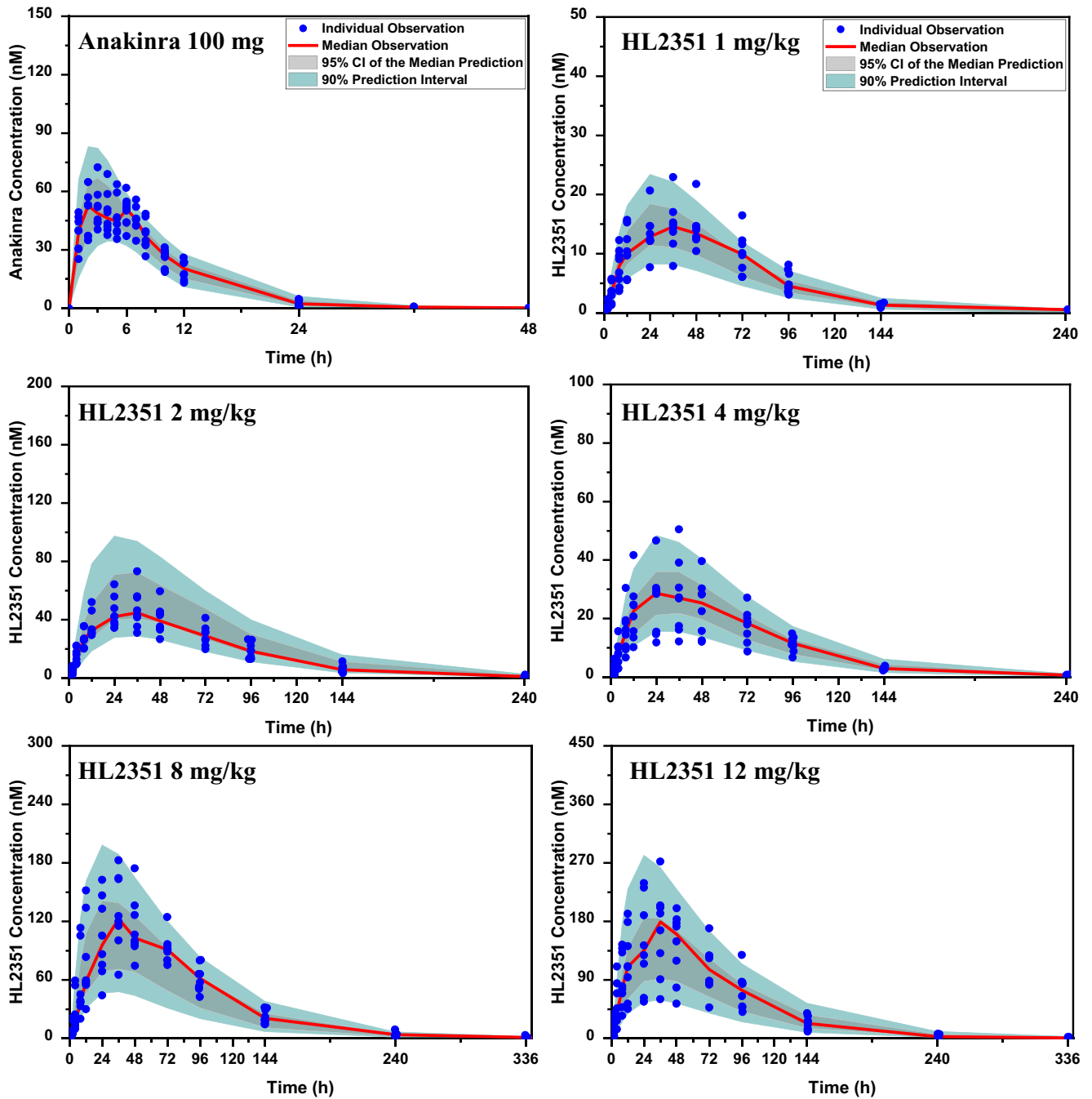
Figure 2 Visual predictive checks for final models regarding observed concentrations of anakinra and HL2351. Open circles represent observed concentrations. The red line represents the observed median, light gray area represents the 95% confidence interval (CI) of the simulated median, and light blue represents 90% prediction interval of simulations.

and coefficient variations of $\overline{C_{b\_ss}}$ are listed in **Table 2**. The relationship between administered dose and $\overline{C_{b\_ss}}$ of HL2351 was fitted well in accordance with the Hill equation (**Figure 3b**), represented by Eqs. 9 and 10.

For HL2351 once weekly $\overline{C_{b\_ss}} = 2.140 \times \dfrac{\text{Dose}^{0.962}}{2.288^{0.962} + \text{Dose}^{0.962}}$

$$(9)$$

For HL2351 once biweekly $\overline{C_{b\_ss}} = 2.145 \times \dfrac{\text{Dose}^{0.726}}{9.681^{0.726} + \text{Dose}^{0.726}}$

$$(10)$$

Accordingly, the HL2351 dosage regimen that mimicked the therapeutic actions of anakinra at each indication for the treatment of RA, CAPS, and Still's disease was estimated. HL2351 at doses of 326 mg or 4.267, 4.982, 5.288, 5.458, or 5.748 mg/kg once weekly or HL2351 at 1726 mg

or 21.92, 26.86, 29.10, 30.36, or 32.53 mg/kg once biweekly could mimic the therapeutic effects of anakinra at a dose of 100 mg or 1, 2, 3, 4, or 8 mg/kg administered once daily (**Table 2** and **Table 3**). The concentration-time curves of anakinra (administered once daily at its therapeutic doses) and those of the respective HL2351 doses (administered once weekly or once biweekly) at steady-state conditions were also simulated (**Figure 4**.)

DISCUSSION

PopPK model for HL2351 and anakinra

An integrated TMDD and FcRn-mediated recycling PopPK model was developed to describe the PK of HL2351. This model was based on the interaction of HL2351 with FcRn via the IgG4-source Fc portion (which explains its longer half-life) and the interaction of HL2351 with its therapeutic target IL1R (which explains its therapeutic effects and distribution). In contrast, anakinra is a recombinant protein that does not consist of the IgG4 source Fc portion, and consequently the PK of anakinra are not significantly affected by the FcRn-mediated recycling; thus a TMDD PopPK model without the FcRn-mediated recycling was developed for anakinra.

Similar to other mAbs, s.c. delivery of HL2351 involves an absorption process from the injection site through the interstitial space and into the lymphatic system before draining into systemic circulation.[36,37] Unlike small molecules, mAbs are primarily eliminated via catabolism. Thus, because of its large size and physicochemical properties, negligible amounts are removed via biliary and renal excretions. The uptake of mAbs into catabolic cells occurs either through pinocytosis at endothelial cells that line the blood vessels (unspecific fluid-phase endocytosis) or by receptor-mediated endocytosis (via either Fc or Fab domains). Because human endothelial cells have large (>1000 m^2) surface areas, pinocytosis substantially contributes significantly to the intracellular uptake and subsequent elimination of mAbs.

FcRn is expressed in vascular endothelial cells in a wide variety of tissues and is exploited as a mechanism to specifically protect IgG and IgG-source Fc fusion mAbs from catabolism.[8–13] FcRn has a low affinity for IgG at a physiological pH, but a high affinity at an acidic pH. Therefore, when mAbs and FcRn are taken up together into the catabolic cell and the endosome is acidified, IgG attaches to FcRn via a specific binding site in the Fc domain. Subsequently, the FcRn–IgG complex is trafficked to the cell surface where the IgG molecule from the complex is released back to the circulation after physiological pH is reached.[8–15] IgG molecules that are not bound to FcRn are catabolized. Thus, IgG has a considerably longer $t_{1/2}$ (~3 weeks) compared with other immunoglobulins and proteins of similar molecular weight (5.8 days for immunoglobulin A, 5.1 days for immunoglobulin M, 2.8 days for immunoglobulin D, and 2.5 days for immunoglobulin E).[16–22] In addition to the interactions with FcRn, the interaction of mAb with its pharmacological target allows it to contribute significantly to the mAb distribution.

The absorption of HL2351 was simulated from beginning at the injection site ($K_{a1} \rightarrow K_{a2}$) to the interstitial space, the lymphatic system, and finally to the systemic circulation. The pathway $K_{SS1} \rightarrow K_{rec}$ models how HL2351 avoids catabolism because of its interactions with FcRn via the IgG4-source Fc portion. In particular, the pathway $K_{a1} \rightarrow K_{SS1} \rightarrow K_{rec}$ models the presystemic catabolism by which HL2351 is transported through the lymphatic system to reach the systemic circulation; $K_{up} \rightarrow K_{SS1} \rightarrow K_{rec}$ models the systemic catabolism of HL2351. The pathway $K_{SS2} \rightarrow K_{deg2}$ models the interaction between HL2351 and its therapeutic target ILIR.

A full TMDD model was first described by Mager and Jusko.[31] However, it may be difficult to identify all parameters of a full TMDD model from the observed PK data because binding reactions occur much more rapidly than other processes ($t_{1/2}$ ranging from minutes to hours compared with $t_{1/2}$ ranging from days to weeks).[32] Therefore, the sampling times typically do not provide sufficient information to estimate binding parameters, particularly when only unbound or total drug concentrations are observed. As such, some parameters of the system are fixed with literature values.[32]

In the present study, a variety of simplification approximations has been applied. First, the QSS approximation model that assumes a balance between binding and sum of the complex dissociation and internalization was used to model the interactions between HL2351 and its targets. Second, K_{up} and K_{deg2}/K_{degA} were set to 0.00952 and 0.206 hour^{-1}, respectively, based on estimations from data reported previously.[38–40] Third, the total amounts (bound and unbound to the drug) of the targets (A_{FcRn_t} and C_{IL1R_t}/C_{IL1R_tA}) were assumed to be constant with no consideration regarding the presence of mAbs. This assumption holds when the degradation rates of the bound and unbound receptor are the same, which is valid in this investigation (as previously discussed[31]). Last but not least, the competition between HL2351 (exogenous IgG) and endogenous IgG for binding to FcRn was not included.

In detail, K_{up} was extracted from the elimination rate constant of IgG in patients with hypercatabolic hypoproteinemia who lacked FcRn functions to recycle IgG.[38] After cellular uptake, IgG can be degraded and eliminated from the body without FcRn-mediated recycling. Consequently, the elimination of IgG from the plasma represents the uptake of mAbs into catabolic cells. In that study, IgG was reported with a mean survival $t_{1/2}$ of 3.033 days. The degradation rate constant K_{deg2}/K_{degA} was extracted from **Figure 2** in the study by Mizel *et al.*[39] using the WebPlotDigitizer tool.[40] They were assumed to be equal to each other and the internalization rate constant of IL1R–IL1.

Given that the average serum level of endogenous IgG in normal individuals is 11.2 g/L (range, 4–22 g/L; equal to ~74,700 nM), which is much higher than the exogenous IgG-source molecules following the administration of IgG mAbs at therapeutic doses.[34,41,42] The maximum concentration of HL2351 in the present study is 272 nM that corresponds to ~0.36% of the endogenous IgG. The presence of HL2351 is, therefore, unlikely to affect substantially the saturation level of FcRn; accordingly, the total amount of FcRn presenting the capacity for binding to IgG seems to change negligible regarding the presence of HL2351. For the same reason, the

(a)

Anakinra once daily

HL2351 once weekly

HL2351 once biweekly

(b)

	HL2351 once weekly	HL2351 once biweekly
Equation	$\overline{C_{b\_ss}} = C_{max} \times \dfrac{Dose^n}{Dose_{50}{}^n + Dose^n}$	
C_{max} (nM)	2.140 ± 0.0147	2.145 ± 0.0564
$Dose_{50}$ (mg/kg)	2.288 ± 0.0407	9.681 ± 0.797
n	0.962 ± 0.0140	0.726 ± 0.0210
R^2	0.9999	0.9998
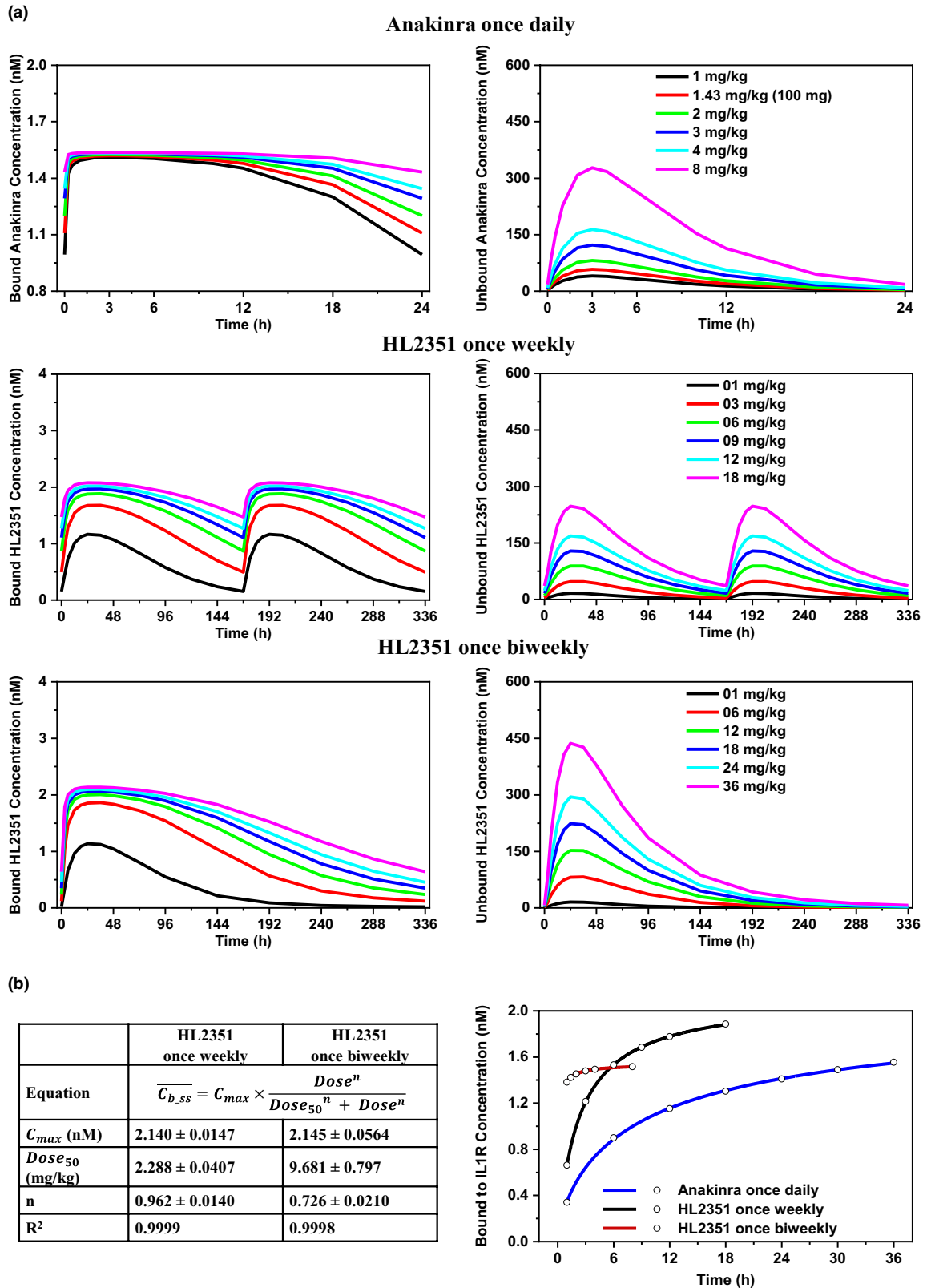
Figure 3 Simulated concentration-time curves and dose-dependent profiles of anakinra and HL2351 in humans following multipledoses at steady-state conditions. (**a**) Concentration-time curves of anakinra and HL2351 bound to IL1R (left) and unbound to IL1R (right) during one dosing interval. (**b**) Relationship between administered dose and average concentrations of anakinra and HL2351 bound to IL1R. Open circles: simulated concentrations, solid lines: regression lines fitted to the simulated concentrations. All notations are defined in the text.

Table 2 Simulated average serum concentrations of anakinra and HL2351 bound to IL1R during one dosing interval at steady-state condition $\overline{C}_{b\_ss}$ following administration of multiple doses in humans and determined dosage regimen for HL2351 (*n* = 1000 replicates)

$\overline{C}_{b\_ss}$(mean and CV)									Determined dosage regimen for HL2351	
Anakinra (once daily)			HL2351 (once weekly)			HL2351 (once biweekly)			HL2351 (once weekly) (mg/kg)	HL2351 (once biweekly) (mg/kg)
Dose (mg/kg)	$\overline{C}_{b\_ss}$(nM)	CV (%)	Dose (mg/kg)	$\overline{C}_{b\_ss}$(nM)	CV (%)	Dose (mg/kg)	$\overline{C}_{b\_ss}$(nM)	CV (%)		
1	1.382	4.86	1	0.6627	13.1	1	0.3412	13.0	4.267	21.92
1.429[a]	1.423	4.05	3	1.214	12.8	6	0.8994	15.4	4.659	24.65
2	1.453	3.33	6	1.532	11.4	12	1.152	15.8	4.982	26.86
3	1.479	2.58	9	1.685	10.1	18	1.303	15.6	5.288	29.10
4	1.494	2.13	12	1.777	9.11	24	1.410	15.2	5.458	30.36
8	1.516	1.30	18	1.885	7.73	36	1.554	14.2	5.748	32.53

CV, coefficient variation.
[a]Pharmacokinetic data were collected at week 5 for anakinra and week 29 for HL2351 postadministration to ensure steady-state conditions.

Table 3 Suggested dosage regimen for HL2351 that mimicked the therapeutic actions of anakinra for the treatment of RA, CAPS, and Still's disease (the drug is administered via subcutaneous injection)

Indication	Dose once 1 week	Dose once 1 week (mg/kg/day)
RA	■ 326 mg	■ 1726 mg
CAPS	– Starting dose: 4.267–4.982 mg/kg – Maintain dose: ■ 5.288–5.458 mg/kg ■ Can be adjusted to a maximum of 5.748 mg/kg	– Starting dose: 21.92–26.86 – Maintain dose: ■ 29.10–30.36 mg/kg ■ Can be adjusted to a maximum of 32.53
Still's disease	– Starting dose ■ BW ≥ 50 kg: 326 mg ■ BW < 50 kg: 5.288–5.458 mg/kg	– Starting dose ■ BW ≥ 50 kg: 1726 mg ■ BW < 50 kg: 29.10–30.36 mg/kg

BW, body weight; CAPS, cryopyrin-associated periodic syndrome; RA, rheumatoid arthritis.

total amount of FcRn presenting the capacity for binding to HL2351 A_{FcRn_t} also seems to change negligible regardless the change in HL2351 concentration over time. As a result, A_{FcRn_t}[43] was assumed to be constant in our model. Significantly, A_{FcRn_t} does not match the amount of FcRn having the capacity for binding to IgG. By estimating the specific amount of FcRn for binding to HL2351, the model indirectly accounted for the competition between HL2351 and IgG in binding to FcRn.

According to the developed PopPK model, the median QSS constants for the interactions of IL1R with anakinra or HL2351 are 0.750 nM and 14.5 nM, respectively, consistent with the findings in previous reports.[44,45] The dissociation constants for interactions between IL1Ra and IL1R have been reported as 0.4 ± 0.1 nM[44] and 0.620 ± 0.061 nM;[45] dissociation constants for interactions between IL1Ra fusion proteins and IL1R have been reported as 3.8 ± 0.5 nM and 13.5 ± 2.9 nM.[45]

Dosage regimen for HL2351 administration
The developed PK models were used to simulate the PK profiles of anakinra and HL2351 in humans after s.c. administration at different dosages. Both drugs show dosage proportionality in PK profiles of the unbound form and nonlinearity in PK profiles of the bound IL1R form (**Figure 3a**). In particular, when the administered dose of anakinra or HL2351 increases, IL1R–D_A or IL1R–D increases exposure in accordance with the Hill equation. The ability of the Hill

function to characterize these data is expected as the Hill function is widely used to describe binding equilibria in ligand-receptor interactions.[46–48]

HL2351 was absorbed slowly and steadily (mean T_{max} of 36 hours) and remained in the body for 240 to 336 hours postadministration. The mAb remained in the body ~7-fold to 10-fold longer (as represented by the mean $t_{1/2}$ and mean residence time) compared with anakinra.[29] Anakinra is administered once daily; therefore, HL2351 was anticipated to be administered once weekly or once biweekly. The average serum concentrations of anakinra and HL2351 bound to IL1R ($\overline{C}_{b\_ss}$) were used for the dosage regimens because binding to IL1R is the mechanism of action of both drugs. The assumption was that if the $\overline{C}_{b\_ss}$ of HL2351 reaches the $\overline{C}_{b\_ss}$ of anakinra, HL2351 would have therapeutic effects similar to those of anakinra. Because of a nonlinearity in PK profiles in the HL2351 bound to IL1R (**Figure 3** and **Table 2**), in cases of dose and dosing frequency of HL2351 to be calculated, it should be calculated using the fitting equation.

Study limitations
This study had some limitations. First, the study was performed in healthy participants, who may not accurately represent patient populations with autoimmune diseases. Therefore, the PK properties of HL2351 obtained from this study may differ from those in real patient populations. However, the longer half-life of HL2351 in the body,
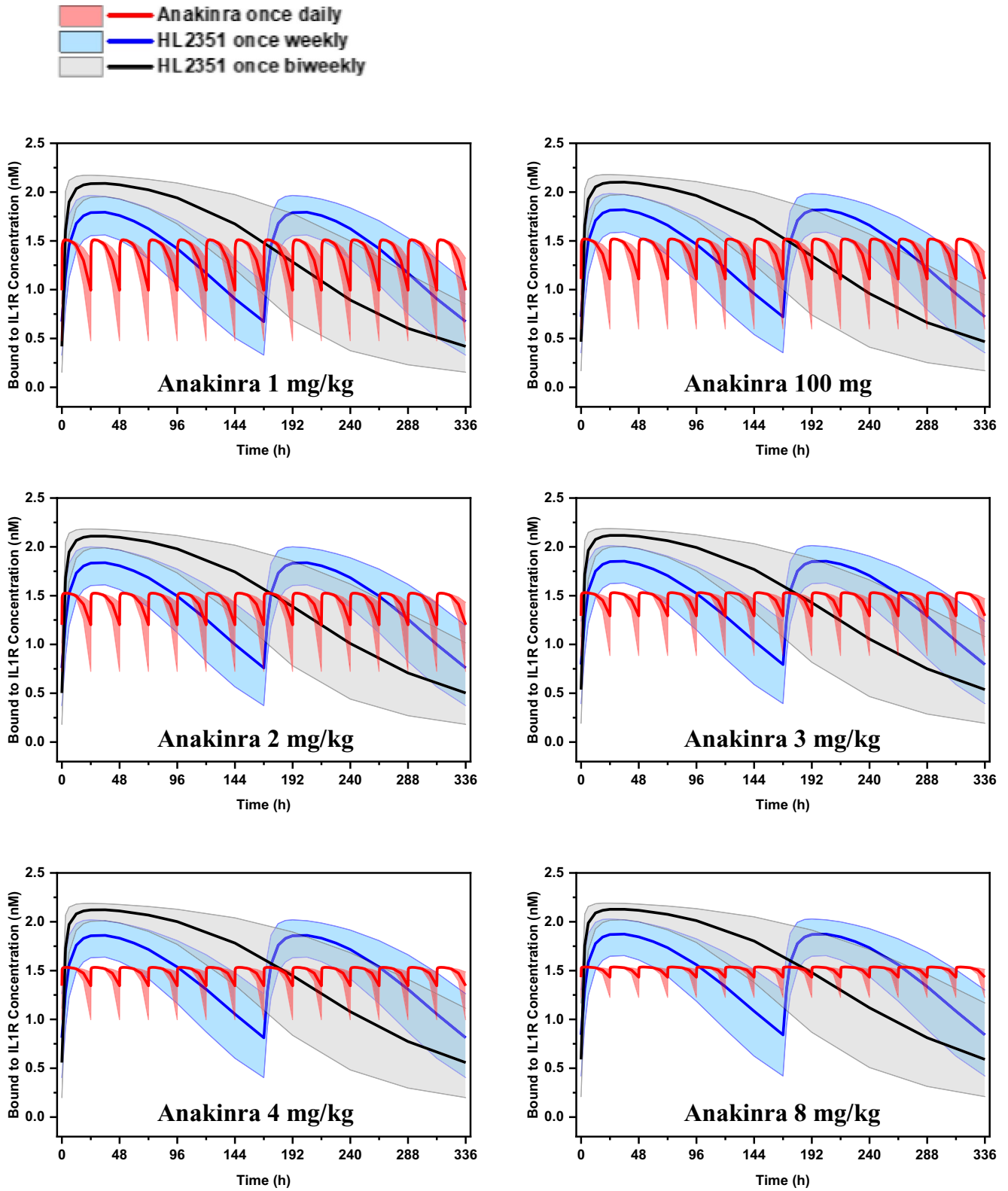
Figure 4 Simulated pharmacokinetics of anakinra (once daily) and corresponding pharmacokinetics of HL2351 (once weekly or once biweekly) at doses where HL2351 mimics the therapeutic effects of anakinra. Lines represent mean concentrations of the population, and areas represent the 90th prediction intervals of population concentrations. IL1R, interleukin-1 receptor.

FcRn-Mediated PK Model and Dosage Regimen for HL2351
Ngo et al.

594

compared with anakinra, is likely to be unaffected by disease status. Second, the PK profiles of HL2351 and anakinra were simulated using a model-based approach. Differences in PK parameters between single-dose and multiple-dose regimens of anakinra and HL2351 were therefore not considered. However, our studies have demonstrated that the observed total serum concentrations of HL2351 (bound and unbound concentrations) are proportional up to a dose of 12 mg.[29] Thus, the linear PK profile of HL2351 total concentration is unlikely to vary following the administration of multiple doses once weekly at the dose range tested. For dosage regimens administered once biweekly, the suggested doses for HL2351 (up to 32.53 mg/kg) are above the dose range tested; thus, the PK profile of HL2351 at a larger dose range should be investigated to ensure the linearity. In summary, further clinical studies should be conducted to determine appropriate doses and dosing intervals for HL2351 in patients with RA, CAPS, or Still's disease.

CONCLUSION

An integrated TMDD and FcRn-mediated recycling PopPK model and a TMDD PopPK model have been developed to describe the individual PK profiles of HL2351 and anakinra in humans after a single s.c. dose. Accordingly, PK profiles of these drugs were simulated following multiple doses in humans. The dose and dosing interval for HL2351, which were 326 mg or 4.267, 4.982, 5.288, 5.458, or 5.748 mg/kg administered once weekly or 1726 mg or 21.92, 26.86, 29.10, 30.36, or 32.53 mg/kg administered once biweekly, were suggested to have therapeutic effects similar to those of anakinra at a dose of 100 mg or 1, 2, 3, 4, or 8 mg/kg administered once daily.

1. Burger, D., Chicheportiche, R., Giri, J.G. & Dayer, J.M. The inhibitory activity of human interleukin-1 receptor antagonist is enhanced by type II interleukin-1 soluble receptor and hindered by type I interleukin-1 soluble receptor. *J. Clin. Invest.* **96**, 38–41 (1995).
2. Platanias, L.C. & Vogelzang, N.J. Interleukin-1: Biology, pathophysiology, and clinical prospects. *Am. J. Med.* **89**, 621–629 (1990).
3. Ren, K. & Torres, R. Role of interleukin-1β during pain and inflammation. *Brain Res. Rev.* **60**, 57–64 (2009).
4. European Medicines Agency Kineret: EPAR - Product Information. <https://www.ema.europa.eu/en/medicines/human/EPAR/kineret> (2019).
5. U.S. Food and Drug Administration Kineret® (anakinra) for injection, for subcutaneous use. Full Prescribing Information for Administration Instructions (2012). <https://www.accessdata.fda.gov/drugsatfda_docs/label/2012/103950s5136lbl.pdf>.
6. Cvetkovic, R.S. & Keating, G. Anakinra. *BioDrugs* **16**, 303–311 (2002).
7. Kaiser, C. *et al.* Injection-site reactions upon Kineret (anakinra) administration: experiences and explanations. *Rheumatol. Int.* **32**, 295–299 (2012).
8. Borvak, J. *et al.* Functional expression of the MHC class I-related receptor, FcRn, in endothelial cells of mice. *Int. Immunol.* **10**, 1289–1298 (1998).
9. Ghetie, V. & Ward, E.S. FcRn: the MHC class I-related receptor that is more than an IgG transporter. *Immunol. Today* **18**, 592–598 (1997).
10. Israel, E.J. *et al.* Expression of the neonatal Fc receptor, FcRn, on human intestinal epithelial cells. *Immunology* **92**, 69–74 (1997).
11. Ghetie, V. *et al.* Abnormally short serum half-lives of IgG in β2-microglobulin-deficient mice. *Eur. J. Immunol.* **26**, 690–696 (1996).
12. Junghans, R.P. & Anderson, C.L. The protection receptor for IgG catabolism is the beta2-microglobulin-containing neonatal intestinal transport receptor. *Proc. Natl. Acad. Sci. USA* **93**, 5512–5516 (1996).
13. Brambell, F.W.R., Hemmings, W.A. & Morris, I.G. A Theoretical Model of γ-Globulin Catabolism. *Nature* **203**, 1352–1355 (1964).
14. Renee, T. & Weilei, M.Analysis of FcRn-antibody interactions on the Octet Platform. <http://www.biophysics.bioc.cam.ac.uk/wp-content/uploads/2011/02/AN_19_FcRn_Antibody_Interactions_Analysis_revB.pdf>.
15. Vaughn, D.E. & Bjorkman, P.J. High-affinity binding of the neonatal Fc receptor to its IgG ligand requires receptor immobilization. *Biochemistry* **36**, 9374–9380 (1997).
16. Lobo, E.D., Hansen, R.J. & Balthasar, J.P. Antibody pharmacokinetics and pharmacodynamics. *J. Pharm. Sci.* **93**, 2645–2668 (2004).
17. Bonilla, F.A. Pharmacokinetics of immunoglobulin administered via intravenous or subcutaneous routes. *Immunol. Allergy Clin. North Am.* **28**, 803–819 (2008).
18. Curtis, J. & Bourne, F.J. Half-lives of immunoglobulins IgG, IgA and IgM in the serum of new-born pigs. *Immunology* **24**, 147–155 (1973).
19. Mankarious, S. *et al.* The half-lives of IgG subclasses and specific antibodies in patients with primary immunodeficiency who are receiving intravenously administered immunoglobulin. *J. Lab. Clin. Med.* **112**, 634–640 (1988).
20. Wang, W., Wang, E.Q. & Balthasar, J.P. Monoclonal antibody pharmacokinetics and pharmacodynamics. *Clin. Pharmacol. Ther.* **84**, 548–588 (2008).
21. Akilesh, S., Christianson, G.J., Roopenian, D.C. & Shaw, A.S. Neonatal FcR expression in bone marrow–derived cells functions to protect serum IgG from catabolism. *J. Immunol.* **179**, 4580–4588 (2007).
22. Chen, Y. & Balthasar, J.P. Evaluation of a catenary PBPK model for predicting the in vivo disposition of mabs engineered for high-affinity binding to FcRn. *AAPS J.* **14**, 850–859 (2012).
23. Xu, C., Su, Y., Paccaly, A. & Kanamaluru, V. Population pharmacokinetics of sarilumab in patients with rheumatoid arthritis. *Clin. Pharma.* **58**, 1455–1467 (2019).
24. Le, K. *et al.* Population pharmacokinetics and pharmacodynamics of lampalizumab administered intravitreally to patients with geographic atrophy. *CPT Pharmacometrics Syst. Pharmacol.* **4**, 595–604 (2015).
25. Mo, G. *et al.* Population pharmacokinetic modeling of olaratumab, an anti-PDGFRα human monoclonal antibody, in patients with advanced and/or metastatic cancer. *Clin. Pharmacokinet.* **57**, 355–365 (2018).
26. Martinez, J.-M. *et al.* Population pharmacokinetic analysis of alirocumab in healthy volunteers or hypercholesterolemic subjects using a michaelis-menten approximation of a target-mediated drug disposition model—support for a biologics license application submission: part I. *Clin. Pharmacokinet.* **58**, 101–113 (2019).
27. Djebli, N. *et al.* Target-mediated drug disposition population pharmacokinetics model of alirocumab in healthy volunteers and patients: pooled analysis of randomized phase I/II/III studies. *Clin. Pharmacokinet.* **56**, 1155–1171 (2017).
28. Kagan, L., Turner, M.R., Balu-Iyer, S.V. & Mager, D.E. Subcutaneous absorption of monoclonal antibodies: role of dose, site of injection, and injection volume on rituximab pharmacokinetics in rats. *Pharm. Res.* **29**, 490–499 (2012).
29. Oh, J. *et al.* Safety, tolerability and pharmacokinetics and pharmacodynamics of HL2351, a novel hybrid Fc-fused IL-1 receptor antagonist, in healthy subjects: a first-in-human study. *Br. J. Clin. Pharmacol.* bcp.14161 (2019). https://doi.org/10.1111/bcp.14161.
30. ThermoFisher Scientific overview of ELISA <https://www.thermofisher.com/kr/ko/home/life-science/protein-biology/protein-biology-learning-center/protein-biology-resource-library/pierce-protein-methods/overview-elisa.html>.
31. Mager, D.E. & Jusko, W.J. General pharmacokinetic model for drugs exhibiting target-mediated drug disposition. *J. Pharmacokinet. Pharmacodyn.* **28**, 507–532 (2001).

32. Gibiansky, L., Gibiansky, E., Kakkar, T. & Ma, P. Approximations of the target-mediated drug disposition model and identifiability of model parameters. *J. Pharmacokinet. Pharmacodyn.* **35**, 573–591 (2008).

33. Ma, P. Theoretical considerations of target-mediated drug disposition models: simplifications and approximations. *Pharm. Res.* **29**, 866–882 (2012).

34. Dua, P., Hawkins, E. & van der Graaf, P. A tutorial on target-mediated drug disposition (TMDD) models. *CPT Pharmacometrics Syst. Pharmacol.* **4**, 324–337 (2015).

35. Keizer, R.J., Karlsson, M.O. & Hooker, A. Modeling and simulation workbench for NONMEM: Tutorial on Pirana, PsN, and Xpose. *CPT Pharmacometrics Syst. Pharmacol.* **2**, e50 (2013).

36. Zhao, L., Ji, P., Li, Z., Roy, P. & Sahajwalla, C.G. The antibody drug absorption following subcutaneous or intramuscular administration and its mathematical description by coupling physiologically based absorption process with the conventional compartment pharmacokinetic model. *J. Clin. Pharmacol.* **53**, 314–325 (2013).

37. Zhao, L., Li, N. & Yang, H. A new stochastic approach to multi-compartment pharmacokinetic models: probability of traveling route and distribution of residence time in linear and nonlinear systems. *J. Pharmacokinet. Pharmacodyn.* **38**, 83–104 (2011).

38. Waldmann, T.A. & Terry, W.D. Familial hypercatabolic hypoproteinemia. A disorder of endogenous catabolism of albumin and immunoglobulin. *J. Clin. Invest.* **86**, 2093–2098 (1990).

39. Mizel, S.B., Kilian, P.L., Lewis, J.C., Paganelli, K.A. & Chizzonite, R.A. The interleukin 1 receptor. Dynamics of interleukin 1 binding and internalization in T cells and fibroblasts. *J. Immunol.* **138**, 2906–2912 (1987).

40. WebPlotDigitizer <https://automeris.io/WebPlotDigitizer/>.

41. Ryman, J.T. & Meibohm, B. Pharmacokinetics of monoclonal antibodies. *CPT Pharmacometrics Syst. Pharmacol.* **6**, 576–588 (2017).

42. Gonzalez-Quintela, A. *et al.* Serum levels of immunoglobulins (IgG, IgA, IgM) in a general adult population and their relationship with alcohol consumption, smoking and common metabolic abnormalities. *Clin. Exp. Immunol.* **151**, 42–50 (2007).

43. Yuan, D., Rode, F. & Cao, Y. A minimal physiologically based pharmacokinetic model with a nested endosome compartment for novel engineered antibodies. *AAPS J.* **20**, 48 (2018).

44. Jerabek-Willemsen, M. *et al.* MicroScale Thermophoresis: Interaction analysis and beyond. *J. Mol. Struct.* **1077**, 101–113 (2014).

45. Shamji, M.F. *et al.* Development and characterization of a fusion protein between thermally responsive elastin-like polypeptide and interleukin-1 receptor antagonist: Sustained release of a local antiinflammatory therapeutic. *Arthritis Rheum.* **56**, 3650–3661 (2007).

46. Gesztelyi, R. *et al.* The Hill equation and the origin of quantitative pharmacology. *Arch. Hist. Exact Sci.* **66**, 427–438 (2012).

47. Attie, A.D. & Raines, R.T. Analysis of receptor-ligand interactions. *J. Chem. Educ.* **72**, 119 (1995).

48. Santillán, M. On the use of the hill functions in mathematical models of gene regulatory networks. *Math. Model. Nat. Phenom.* **3**, 85–97 (2008).